XX IMEKO World Congress
Metrology for Green Growth
September 9–14, 2012, Busan, Republic of Korea

NUMERICAL STUDY ON THE EFFECT OF LOW REYNOLDS NUMBER FLOWS IN STRAIGHT TUBE CORIOLIS FLOWMETERS

Rongmo Luo [a], *Jian Wu* [a], *and Steven Wan* [b]

[a] National Metrology Centre, A*STAR, 1 Science Park Drive, Singapore 118221;
[b] Institute of High Performance Computing, 1 Fusionopolis Way, #16-16 Connexis North, Singapore 138632

Abstract: A numerical model has been developed to simulate the single straight tube Coriolis mass flowmeters (CMFs), to study the vibration mode shape of the sensor tube for mass flow rate measurement. In this model, a finite volume (FV) code for fluid flow analysis and a finite element (FE) code for structural analysis are coupled based on the theories of fluid-structure interaction. The effect of the low Reynolds number on the sensitivity of CMF has been studied in details, and the simulation results can gain a deeper understanding of the error behaviour of CMFs under high viscous flow.

Keywords: Coriolis mass flow meter; Lower Reynolds number; High viscosity flow; Fluid-structure interaction.

1. INTRODUCTION

As one of the high-precision devices to directly measure the mass flow of fluid, CMFs are currently one of the most rapidly developed flowmeters and has the potential for wide applications in the future [1].

In the measuring line, real process conditions may cause a CMF to deviate from the ideal linear behaviour mainly due to coupled dynamics of fluid and structure [2]. The disturbance conditions include entrained air-bubbles, line pressure drop, change in the compressibility of the fluid, and extremely low Reynolds number (Re) flow. The Re number of flow in a CMF can be estimated by mass flows and tube damping information. Recently, plenty of applications and increasing interests are found for fluid-structure interaction (FSI) with coupled computational fluid mechanics (CFD) and computational structural mechanics (CSM) in industries, including flow measurements devices.

In the present study, a finite volume (FV) code for fluid flow analysis and a finite element (FE) code for structural analysis are coupled to simulate the single straight tube Coriolis mass flowmeters (CMFs) based on the theories of fluid-structure interaction. The effect of the low Reynolds number on the sensitivity of CMF was studied in details.

2. MATHEMATICAL MODELS

The fluid-conveying measuring sensor tube in the Coriolis mass flowmeter is maintained to vibrate periodically at its natural frequency under impulsively forced vibration conditions (resonance). Mass flow is usually measured as the time or phase difference between the motion of two sensing points on the tube, which are positioned symmetrically along the tube length. However, the distortion of symmetry of the no-flow drive mode is resulted from the interaction between the motion of the tube and the fluid flow due to the CMF's inertial force field, where the straight measuring tube is clamped at both ends and vibrating at its first natural frequency. This section presents the governing equations and corresponding general boundary/initial conditions which we have used in the present simulations.

2.1 Fluid domain

The conservation equations of mass and momentum are written in the integral form for the three-dimensional spatial distribution and time range ($t > 0$) of fluid flow as

$$\frac{\partial}{\partial t}\int_{\Omega_F} \rho_F d\Omega + \int_{\Gamma_F} (\mathbf{V}_F - \mathbf{V}_S)\cdot \mathbf{n} d\Gamma = 0 \quad (1)$$

$$\frac{\partial}{\partial t}\int_{\Omega_F} \rho_F \mathbf{V}_F d\Omega + \int_{\Gamma_F} \rho_F \mathbf{V}_F (\mathbf{V}_F - \mathbf{V}_S)\cdot \mathbf{n} d\Gamma = \int_{\Gamma_F} \boldsymbol{\sigma}_F \cdot \mathbf{n} d\Gamma + \int_{\Omega_F} \mathbf{f}_F d\Omega \quad (2)$$

where movement of fluid flow with the density $\rho_F(x,t)$ and the velocity $V_F(x,t)$ in the domain Ω_F ($x \in \Omega_F$) are influenced by the motion of a surrounding boundary velocity v_s. The vector $\mathbf{f}_F(x,t)$ in the momentum equation (2) is the volume forces acting inside the domain Ω_F, and $\sigma_F(x,t)$ is the resulting tensor.

The respective boundary conditions can be written as

$$\begin{aligned}
&\mathbf{V}_F(x,t) = \mathbf{V}_{\text{inflow}}, \ x \in \Gamma_{\text{inflow}}, \\
&p_F(x,t) = p_{\text{outlow}}, \ x \in \Gamma_{\text{outflow}}, \\
&\mathbf{V}_F(x,t) = v_s(x,t), \ x \in \Gamma^m_{\text{tube}}(t), \\
&\mathbf{V}_F(x,t) = 0, \ x \in \Gamma^{in}_{\text{tube}}(t) \vee x \in \Gamma^{out}_{\text{tube}}(t),
\end{aligned} \quad (3)$$

where $\mathbf{V}_{\text{inflow}}$ is the inflow fluid velocity, Γ is the fluid boundary, p_{outflow} is the absolute fluid pressure at fluid outflow, and $v_s(x,t)$ is the velocity of the measuring tube surface.

2.2 Structure domain

The conservation of momentum principles is utilized for the three-dimensional spatial distribution ($x \in \Omega_s$) and time evolution ($t > 0$) of the structural response, where the

respective equation of motion can be derived by Hamilton's variational principle,

$$\int_{t_1}^{t_2} \delta(W_P - W_k)dt = 0 \tag{4}$$

where W_p and W_K are the total potential energy and the total kinetic energy of the moving solid structure, respectively. The detailed expressions for them are defined as [3],

$$W_P = \frac{1}{2}\int_{\Omega_s} \sigma_s : \varepsilon_s d\Omega - \int_{\Gamma_s} \mathbf{P}_s \cdot \mathbf{u}_s d\Gamma - \mathbf{F}\cdot\mathbf{r}_P \tag{5}$$

$$W_k = \frac{1}{2}\int_{\Omega_s} \rho_s(\mathbf{v}_s \cdot \mathbf{v}_s)d\Omega \tag{6}$$

where the surface tractions $\mathbf{P}_s(x,t)$ acting upon the moving shell boundary through the respective displacement field $\mathbf{u}_s(x,t)$, and the concentrated force $\mathbf{F}(t)$ at point P, where the forced vibration is generated. $\varepsilon_s(x,t)$ and $\sigma_s(x,t)$ are the strain and the stress tensor in the shell structure, and $\mathbf{r}_P$ is the position vector of point P where the force $\mathbf{F}$ is applied. $\rho_s(x,t)$ is the structure material density and $\mathbf{v}_s(x,t)$ is the structure velocity field.

At $t=0$, the initial velocity and acceleration fields, $\mathbf{v}_s(x,0)$ and $\mathbf{a}_s(x,0)$ must be given, and $\sigma_s(x,0)=\varepsilon_x(x,0)=0$. At $t>0$,

$$\mathbf{u}_s(x,t)=0,\ x\in\Gamma^u_{\text{tube}},$$
$$\boldsymbol{\sigma}_s(x,t)\cdot\mathbf{n}(x,t)=\mathbf{P}_s(x,t),\ x\in\Gamma^u_{\text{tube}}(t),$$
$$\mathbf{F}(t)=(\mathbf{F}(t),0,0),\ x=x_P \tag{7}$$

For the structural-side boundary conditions, the sensing tube was fixed at both ends. In order to simulate the tube exciter, a periodic or harmonic force was applied at the center of tube point P. The first frequency of the sensing tube (the drive frequency of the meter) is equal to the frequency of the oscillating force. A periodic force was applied at the centre Point P to oscillate the pipe in the x-direction,

$$\mathbf{F}(t)=(F_0\sin(2\pi n f_d \Delta t),0,0) \tag{8}$$

where Δt is the integration time step, f_d denotes the drive frequency, and F_0 represents the amplitude of the periodic force.

2.3 Method of analysis

The present simulation uses the ANSYS Workbench framework employing DesignModeler, SIMULATION, ANSYS, CFX Mesh and CFX solver. The work flow chart is as shown in Figure 1.

The pipe is created in DesignModeler, with the structural and fluid domain representing the tube wall and the fluid inside the tube. SIMULATION and CFX Mesh are used to mesh the solid and fluid domain, respectively.

To determine the investigated tube's natural frequency, a modal analysis of the solid domain is conducted in ANSYS. The determined natural frequency is used to calculate the excitation force at point P. And then a dynamic response analysis for the solid domain is performed based on the linear elastic theory, where the deformations of the sense tube are assumed to be small. And it can determine the time step for FSI analysis.

To obtain the initial conditions for the transient fluid analysis, a steady state analysis is carried out in CFX over the fluid domain.

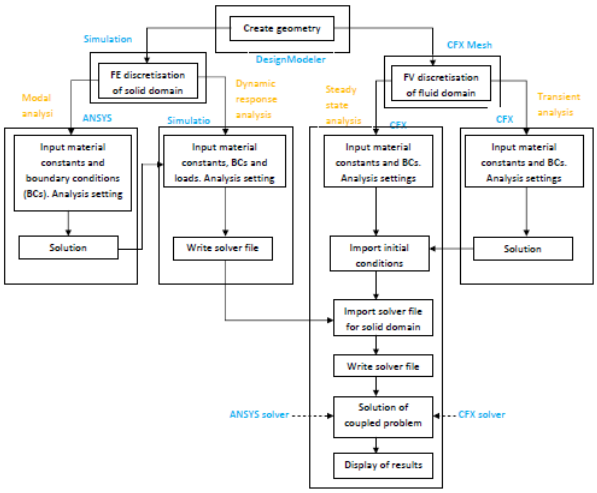

Figure 1. The work flowchart for the ANSYS Workbench framework is used for the present simulation.

The two steady state analyses are employed for the transient analysis of the fluid domain. The FSI analysis is carried out within CFX (ANSYS v13.0).

To obtain equilibrium conditions at the fluid-structure boundary, the stagger-iterations procedure is needed for each coupling time step, as shown in Figure 2. The result of the transient simulation for the fluid domain at the previous time step t_{n-1} is used by the CFX solver as initial condition at time step t_n to determine the load on the tube wall induced by the fluid. The load is then transferred to the solid domain for the boundary condition with the deformation of the tube at the time step t_{n-1}. The motion of the tube wall is calculated and transfer to the fluid domain to update the fluid mesh. The CFX solver determines the load at time step t_{n+1} on the tube wall using the updated mesh and fluid data at time step t_n. As the loads transfer across the meshes using the FSI boundary, a globally conservative interpolation method is used to interpolate the load over the meshes.

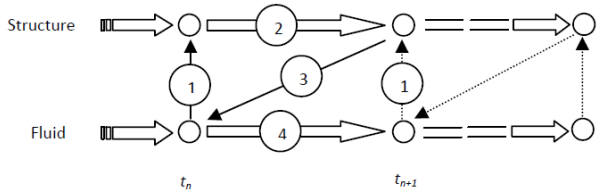

Figure 2. The stagger-iterations procedure is used for the FSI analysis.

During the information transferring, both the kinematic and dynamic constraints are set for the FSI interface,

$$\mathbf{V}_F(x,t_n)|_F = \mathbf{V}_F(x,t_n)|_s$$

$$\mathbf{u}_s(x,t_n)|_s = \mathbf{u}_s(x,t_n)|_F$$
$$F_j^{\mathrm{FSI}} = \int (p\delta_{ij} + \sigma_{ij}) d\Gamma_i^{\mathrm{FSI}} \quad (9)$$

where F_j^{FSI} denotes the total force vector from the CFX solver to the structural solver, and σ_{ij} includes the viscous and turbulent part of the momentum tensors. On the other hand, structural displacements $\mathbf{u}_s(x,t_n)$ are transferred from the structure to the fluid in order to fulfil kinematic constraints.

The 10-15 periods with 400 time-steps are run for the entire FSI simulation and the displacements at two sensor locations have been recorded at each time step, as shown in Figure 3. For a typical case, a computing time of approximately 64 CPU hours is required for fully converged solution for 15 periods. Consequently a signal processing tool is used to find the phase difference between two sensor locations.

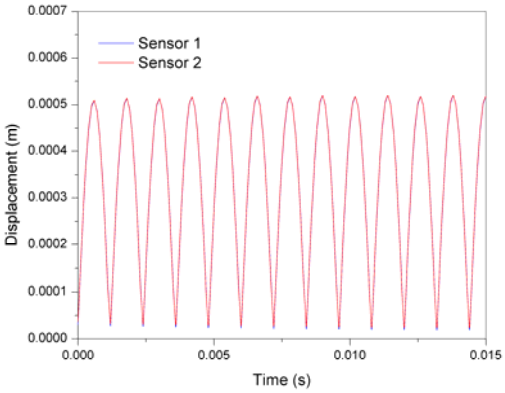

Figure 3. The displacement of sensor 1 and 2.

3. RESULTS AND DISCUSSION

To validate the developed FSI model, the simulation results are compared with the results of the open literature [3]. The resulting model is used to study the effect of the low Reynolds number on the sensitivity of CMF in details.

3.1 Benchmark work

The analysed CMF is characterized by the length $L = 20D$ of a straight measuring part of the tube and a cross-section geometry which is determined by the internal diameter $D = 20$ mm and wall thickness $\delta = D/40$. The distance between the symmetrically positioned sensing points S_1 and S_2 is $L_s = 10D$. The material of the tube is titanium with density 4510 kg/m^3, Young's modulus 102700 MPa and Poisson ratio 0.34. The equivalent stiffness K_{tube} of the measuring tube is 483.5 N/mm. The simulations of the performance of the CMF were carried out for water with $\rho_F = 1000$ kg/m^3 and $\mu = 1\times10^{-3}$ Pa.s and for four different fluid average axial velocities $\mathbf{V}_F = 0.1$, 0.4, 2.0 and 5.0 m/s, respectively.

The FE and FV domain discretization applied to the structural domain and the fluid, respectively, is schematically shown in Figure 4. It consists of 3657 shell type FEs and 67 392 FV cells.

a)

b)

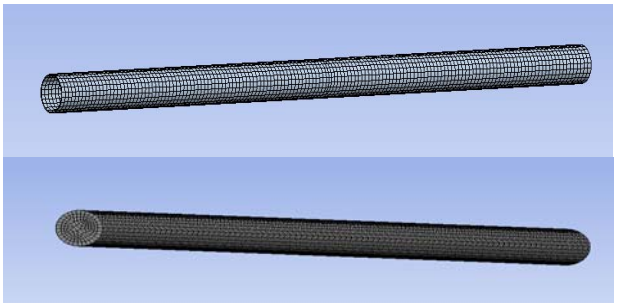

Figure 4. The discretized meshes for a) the structural domain, and b) the fluid domain.

The result obtained from the last 10 periods is further used as the calculated phase difference. Figure 5 represents phase differences for four different axial flow velocities in the measuring tube with comparison to the results of Ref [3]. It is found that the observed phase differences encountered in the considered straight tube CMFs are of order of magnitude lower than one degree, and that the predicted measuring characteristic (variation of the phase difference with the average fluid velocity) of the flowmeter is approximately linear. And the consistent comparison validates the present developed FSI model.

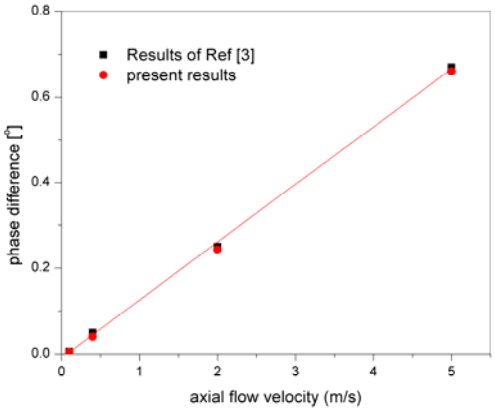

Figure 5. Phase difference between the sensing points S1 and S2 for four different fluid average axial velocities.

3.2 Effect of low Re flow

As mentioned above, the low Re flow may cause measurement deviations, especially significant in the metering of highly viscous fluids. Report and studies from several laboratories and field measurements with certain devices clearly indicate that a shift in the meter calibration factor arises at low Re [2].

The Reynolds number can be obtained for a measuring tube as

$$\mathrm{Re} = \frac{4\dot{m}}{n_t \pi \mu D_i} \quad (10)$$

where $\dot{m}$ is the mass flow, n_t the number of measuring tubes, μ the dynamic viscosity and D_i the inner diameter of the measuring tube.

In the present study, we evaluate the CMF's error by comparing the phase difference ϕ_i of each period of the CMF with the arithmetic mean $\bar{\phi}$ of the phase difference of each period by the percentage error $e_{pi} = \frac{\phi_i - \bar{\phi}}{\bar{\phi}} \times 100\%$, and the sample standard deviation of percentage errors s_{pe} is defined as,

$$s_{pe} = \sqrt{\frac{\sum (e_{pi} - \bar{e}_p)^2}{n-1}} \tag{11}$$

where $\bar{e}_p$ is the arithmetic mean of percentage errors of n repeated periods for a specific Re.

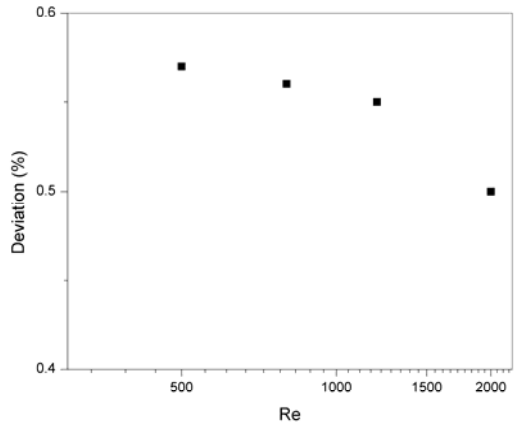

Figure 6. Numerical computed deviation values against Reynolds number.

With the help of coupled FSI simulations, the influence of Reynolds number is simulated and numerical computed phase difference values are plotted in Figure 6, which can be used to compare with the experimental data of the same device. Further study on the numerical simulations qualitatively to support with the experimental observations will be carried out.

4. CONCLUSION

The study presents a FSI model coupled a finite volume (FV) code for fluid flow analysis and a finite element (FE) code for structural analysis to simulate the single straight tube Coriolis mass flowmeters (CMFs). The effect of low Reynolds number on the sensitivity of CMF was studied. Results from coupled fluid-structure numerical simulations, mainly for low Reynolds numbers, help to understand the meter measurement deviations caused by these disturbances at low Reynolds numbers.

5. REFERENCES

[1]. Wang, L. J., Hu, L., Zhu, Z. C., Ye, P., and Fu, X., "Analytical calculation of sensitivity for Coriolis mass flowmeter". Measurement, vol. 44, no. 6, pp. 1117-1127, 2011.

[2]. Kumar, V. and Anklin, M., "Numerical simulations of Coriolis flow meters for low Reynolds number flows". Mapan, vol. 26, no. 3, pp. 225-235, 2011.

[3]. Mole, N., Bobovnik, G., Kutin, J., Stok, B., and Bajsic, I., "An improved three-dimensional coupled fluid-structure model for Coriolis flowmeters". Journal of Fluids and Structures, vol. 24, no. 4, pp. 559-575, 2008.